

Hybrid Photodiode Crosstalk due to Backscattered Electrons

J. Freeman, D. Green and A. Ronzhin

*Fermi National Accelerator Laboratory
P.O.Box 500, Batavia, Illinois 60510*

Abstract. The fraction of backscattering electrons are measured for 19 and 73 pixels Hybrid Photodiodes. The data obtained are in good agreement with calculations. A new method of HPD alignment is proposed and tested.

INTRODUCTION

The Hybrid Photodiode (HPD, [1]) has been chosen to be the photodetector for the Compact Muon Solenoid (CMS) Hadron Calorimeter (HCAL) readout [2]. The HPD will be operating in a 4 Tesla magnetic field that is chosen to be parallel to the HPD electric field. This choice was made in order to reduce crosstalk between pixels of the device. Some effects of the HPD's signal increase were observed first and also explained [3,4,5,6,7] previously for this field orientation. The phenomena are due to backscattered electrons [8]. The new data obtained with both 19 pixel and 73 pixel HPDs are presented below.

Setup

The test setup (Figure 1) consisted of a nitrogen laser (337 nm) illuminating a block of SCSN81 scintillator. The scintillation light was then transported to the HPDs by a 5 meter length, 0.6 mm diameter quartz fiber. The amount of light was monitored by a PIN diode optically attached to the scintillator. The HPDs were installed in a magnet which has poles of diameter 150 cm and a distance between poles of 7 cm. The HPD's optical glass window plane was carefully aligned parallel to the magnet poles plane. The value of the magnetic field was measured with a Tesla meter. Three HPD pixels and the PIN diode were connected to the four inputs of a Tektronics TDS 3054 500 MHz digital oscilloscope by coax cables. The coax cables were terminated into 50 Ohms at the scope input. All other pixels of the tested HPDs were grounded.

Measurements

19 pixels HPD

The HPD schematic view is shown in Figure 2. The distance between photocathode (PC) and silicon (Si) is about 3.35 mm \pm 0.02 mm for the HPD. The value of the high voltage between PC and Si was 10 kV, the Si bias voltage was 80 V in the measurement. The silicon thickness of the HPD is 200 μ m. The pixels of the HPD are shown in Figure 3. The flat-to-flat distance of the hexagon shaped pixel is 5.6 mm. A quartz fiber of 600 μ m diameter was installed in the geometrical center of the central pixel #10 with 30 μ m accuracy.

Measurements were performed for the HPD's linear range response. Only pixel nr. 10 was illuminated. The signals were taken from the pixel and the neighboring pixels nrs. 11 and 12. Data were taken with PIN diode normalization because the observed effects are at the few percent level and the laser light spread was about \pm 7%. The accuracy of the magnetic field measurement was better than 1%. The accuracy of the HPD normal axis alignment relative to the magnet normal axis was better than 3 degrees. Presumably the HPD electric field direction was adjusted parallel to the magnetic field with the same accuracy. The signals from the pixels are shown in Figures 4, 5 and 6. The magnitude of the magnetic field was changed. The main source of noise was due to the laser. The noise data were taken without laser light illuminating the HPD. This noise was subtracted because it kept a constant shape during data taking. The result of the subtraction is shown in Figures 7, 8 and 9. The signals from pixels 11 and 12 were obtained by subtraction of the signals at the highest value of the magnetic field that is 0.5 Tesla in the measurement. The signals are observed after that only for pixels 10 and 11 (Figures 10 and 11). The dependences of peak amplitude on the magnetic field value are shown in Figures 12 and 13 for pixels 10 and 11. No change in the pulse waveform was observed in the measurements (1 ns accuracy).

73 pixels HPD

The 73 pixel HPD schematic view is shown in Figure 14. The flat-to-flat distance is 2.8 mm. All other conditions are the same except that the bias voltage is 130 V and the silicon thickness is 300 μ m for the 73 pixel HPD. The data obtained are shown in the same sequence as for 19 pixel HPD. The signals from the central pixel (nr. 37) and neighboring pixels (nrs. 38 and 39) are shown in Figures 15, 16 and 17. The signals for the highest value of the magnetic field and after laser noise subtraction are presented in Figures 18, 19 and 20. The resulting signals from all the pixels (37, 38 and 39) are clearly observed now. The peak values dependencies on the magnitude of the magnetic field are presented in Figures 21, 22 and 23.

Discussion

The observed effects can be explained with a model of backscattered electrons [8]. The fraction of backscattered electrons is about 18% for 10 KeV kinetic energy photoelectrons. The angular distribution of the backscattered electrons follows a cosine function of the reflection angle. The maximum transverse momentum is 100 keV/c for the 10 KeV elastic photoelectron's scattering. The maximum distance along the silicon surface is 6.7 mm for the backscattered electrons. The photoelectrons can, therefore, only reach pixel 11 of the 19 pixels HPD and pixels 38 and 39 of the 73 pixels HPD (Figure 24). The backscattered electrons focused by the longitudinal magnetic field (Figure 2) results in a redistribution of energy of backscattered electrons toward the central pixel.

Comparison to Data

A simplified model was constructed having a 10 kV accelerating voltage across a 3 mm gap. The angle between the magnetic and electric fields was taken to be zero degrees. For each impact on the silicon, a fixed reflection coefficient of 20% was taken [9]. The backscattered electron angle and kinetic energy were chosen from factorized distributions [9] and propagated in combined electric and magnetic fields to the secondary impact point.

The distance of that point from the initial impact point cannot exceed twice the gap distance or 6 mm. The exact distribution of energy and distance determines the energy of crosstalk to neighboring pixels. The radius distribution at zero magnetic field extends fairly uniformly from zero to 6 mm. Due to ionization losses, the struck pixel typically receives a deposit of ~ 3 keV for backscattered electrons, the remaining ~ 7 keV being given to the kinetic energy of the reflected electron.

The fractional energy with a distance > 2.8 mm was studied for magnetic fields from zero to 0.3 T. Above that field the magnetic field captures all electrons into orbits with a radius smaller than the distance of 2.8 mm. It is assumed that the central pixel was illuminated by a point source, and that the hexagonal boundary could be approximated by a circular one.

The nearest neighbor energy with respect to the central pixel energy for a 19 pixel device varies from 9.5% for no magnetic field to 0% at 0.3 T magnetic field. The falloff is quite linear, and roughly describes the data.

The reflected electrons can reach both nearest and next to nearest neighbors in the case of 73 pixel device. In this case the data was compared to the energy deposited in a central disk, a nearest neighbor annulus, and an outer annulus. As can be seen the central disk again gains $\sim 10\%$ in energy due to the focusing effect of the magnetic field on the backscattered energy. The nearest neighbor pixel first gains energy as the outer radii are pulled into it. With higher fields the energy is refocused

onto the central pixel and the energy going into the annulus falls. For the next to nearest neighbor, the energy falls smoothly and at 0.2 T magnetic field, all the reflected energy is pulled off the pixel by the field.

Therefore, the simple theory of backscattered electrons is confirmed by the new data. The behavior of the central, nearest neighbor and next to nearest neighbor is qualitatively well understood.

Application

The effect of backscattering can be useful in checking the alignment of the HPD along the 4 Tesla magnetic field. The maximum radius of the backscattered electrons is about 50 μm in a 4 Tesla field. It is evident that a measurement of backscattered electrons on neighboring pixels can locate the photoelectron impact point. A single fiber on the boundary between 3 pixels (in the middle of the “Mercedes “ sign) can be installed for the purpose. The misalignment of the HPD electric field to the external longitudinal magnetic field will be manifested as an imbalance of the increase of these 3 signals in the presence of the magnetic field. Very precise positioning of the fiber on the 3 pixel boundary is not needed because the ratio of the signals increase can be used to estimate the magnitude of the misalignment. To check the accuracy of the method a fiber with 600 μm diameter was shifted by 200 μm along the photocathode perpendicular to the flat side of the hexagonal pixel (73 pixels HPD). The observed backscattering signal change was measured to be 100 mkV and 50 mkV for neighboring pixels 38 and 39.

Conclusions

1. The fraction of backscattered electrons measured for 19 pixels and 73 pixels HPDs was measured. It was seen that the crosstalk due to this source is eliminated at high magnetic fields.
2. The data measured are in good agreement with the performed calculations.
3. A new method to check HPD alignment in the longitudinal magnetic field is proposed.

Acknowledgments

We appreciate useful discussion with Robert Tshchirhart, Julia Whitmore and Valery Balbekov.

REFERENCES

1. "Hybrid Photomultiplier Tubes," DEP, Delft Instruments.
2. CMS, The Hadron Calorimeter Technical Design Report, CERN/LHCC 97-31, June 20, 1997.
3. Green, D., "Backscattering in Hybrid Photodetector Devices," Fermilab FN-662, 1997.
4. Freeman, J.; Green, D.; Ronzhin, A., et al. "Test of DEP Hybrid Photodiode in 5 Tesla Magnet," Fermilab TM-2027, 1997.
5. Freeman, J.; Green, D.; Ronzhin, A., "Test of HPD," Report on SCIFI 97, Notre Dame University, Indiana, USA, in the book, SCIFI 97: Conference on scintillating and fiber detectors, AIP Conference proceedings 450, Woodbury, New York, 1998, p.497.
6. Freeman, J.; Green, D.; Ronzhin, A., "Effect of HPD Signal Increase in a Magnetic Field Parallel to the HPD Electric Field," Fermilab TM-2039, 1998.
7. Cushman, P.; Heering, A.; Ronzhin, A. Studies of Hybrid Photomultiplier Tubes in Magnetic Fields Up to 5 Tesla. NIM, A 418, 1998, p.300.
8. Darlington, E., J. Phys. D: Appl. Phys. Vol. 8, 1975, p.85.
9. Green, D., "Simple Theory of Silicon Backscattering," Fermilab-FN-668, 1997.

Figure Captions

1. Setup.
2. 19 pixels HPD schematic view.
3. Pixel's schematic view, 19 pixels HPD.
4. Signals from pixel 10 with and without magnetic field.
5. Signals from pixel 11 with and without magnetic field.
6. Signals from pixel 12 with and without magnetic field.
7. As in Fig. 4 after laser noise subtraction.
8. As in Fig. 5 after laser noise subtraction.
9. As in Fig. 6 after laser noise subtraction.
10. Signals from pixel #10 after subtraction of the "capacitance" crosstalk which was measured at 0.5 Tesla magnitude of the magnetic field.
11. Signals from pixel #11 after subtraction of the "capacitance" crosstalk which was measured at 0.5 Tesla magnitude of the magnetic field.
12. Dependence of the peak signal amplitude, (pixel #10) on the value of the longitudinal magnetic field (measured – closed circles, calculated – open circles).
13. Dependence of the peak signal amplitude, (pixel #11) on the value of the longitudinal magnetic field (measured – closed circles, calculated – open circles).
14. 73 pixels HPD pixel's schematic view, the maximum area of the backscattered electrons is indicated by the circle.
15. Signals from pixel #37 with and without magnetic field.
16. Signals from pixel #38 with and without magnetic field.
17. Signals from pixel #39 with and without magnetic field.
18. Signals from pixel #37 after subtraction of the "capacitance" crosstalk which was measured at 0.5 Tesla magnitude of the magnetic field.
19. Signals from pixel #38 after subtraction of the "capacitance" crosstalk which was measured at 0.5 Tesla magnitude of the magnetic field.
20. Signals from pixel #39 after subtraction of the "capacitance" crosstalk which was measured at 0.5 Tesla magnitude of the magnetic field.
21. Dependence of peak signal amplitude (pixel #37) on the value of the longitudinal magnetic field (measured – closed circles, calculated – open circles).
22. Dependence of peak signal amplitude (pixel #38) on the value of the longitudinal magnetic field (measured – closed circles, calculated – open circles).
23. Dependence of peak signal amplitude (pixel #39) on the value of the longitudinal magnetic field (measured – closed circles, calculated – open circles).

PIXELS 10, 11, 12 terminated by 50 Ohm,
all others pixels terminated on ground.

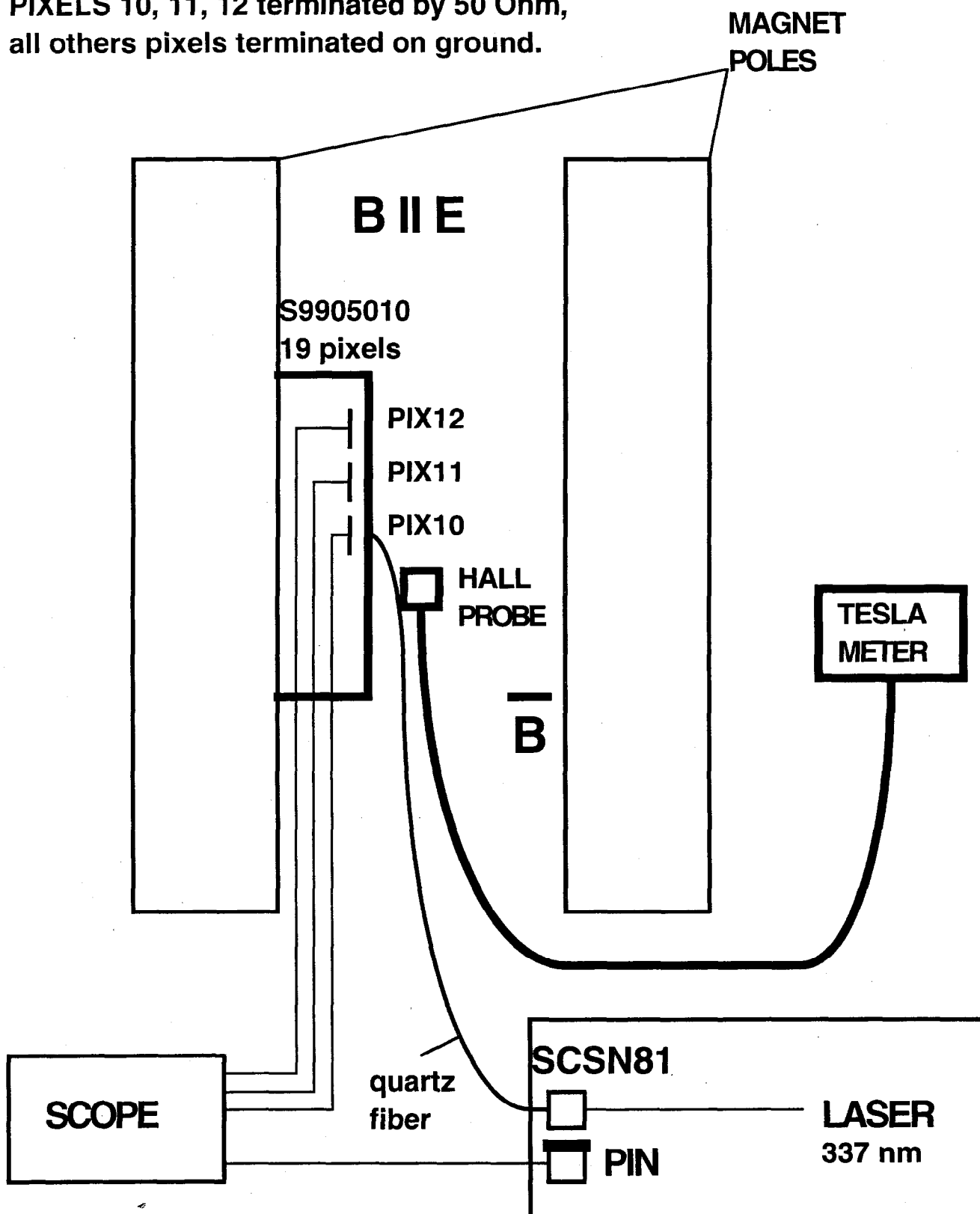


Fig.1

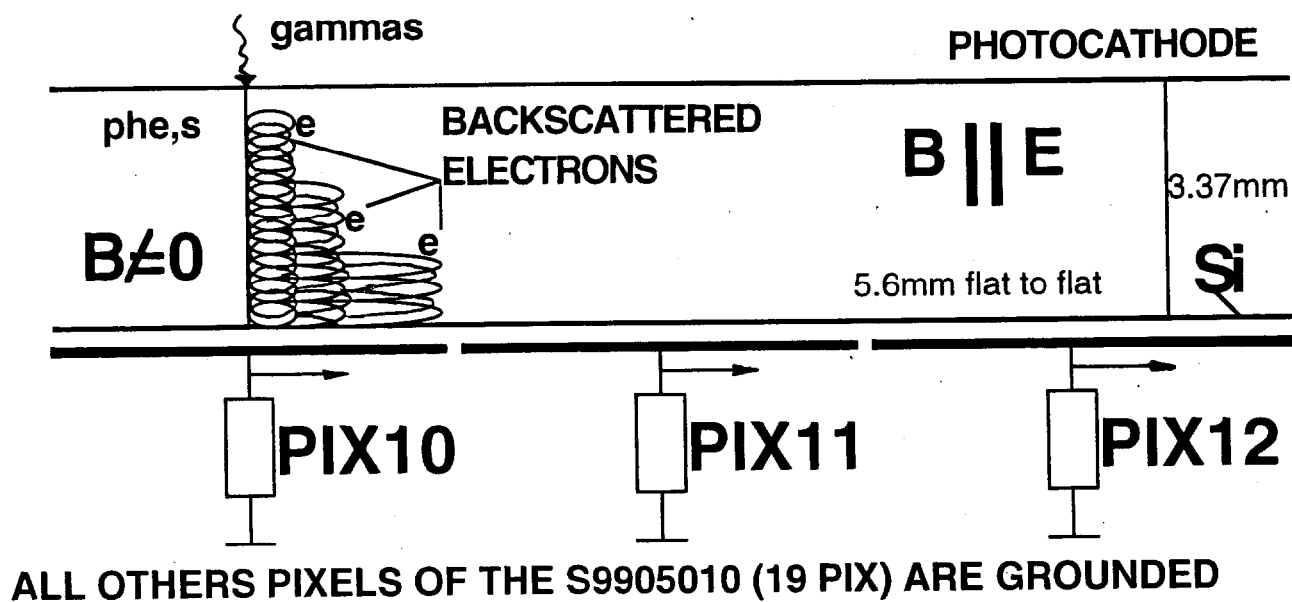
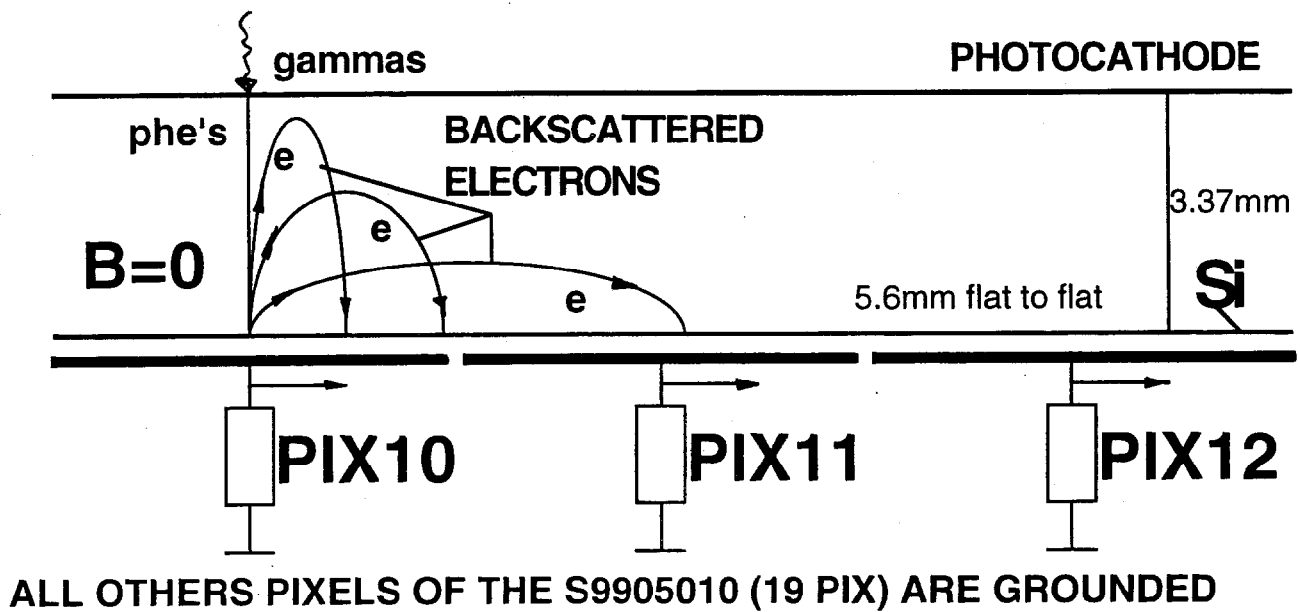


Fig.2

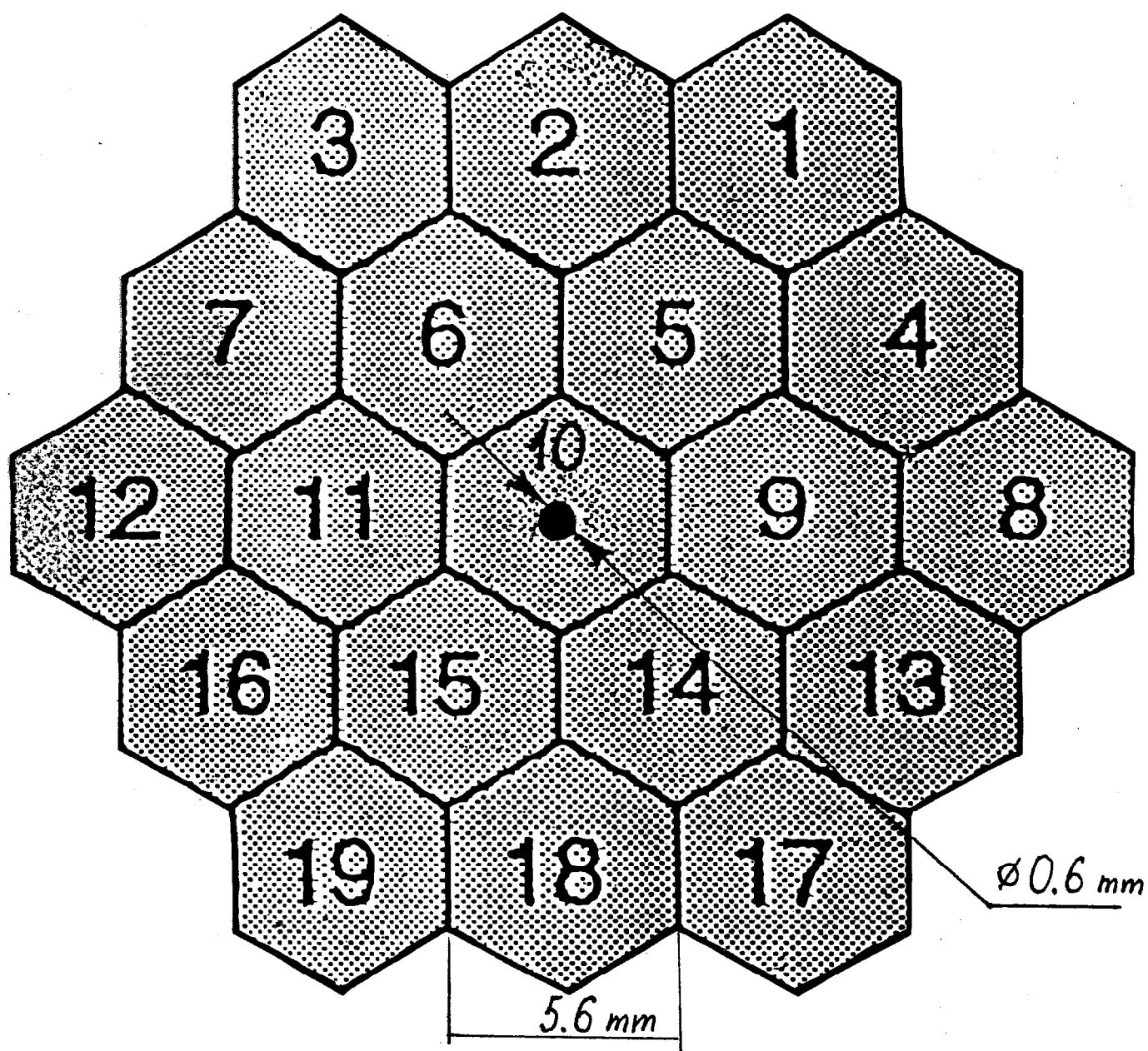


Fig.3

pix 10, B variable

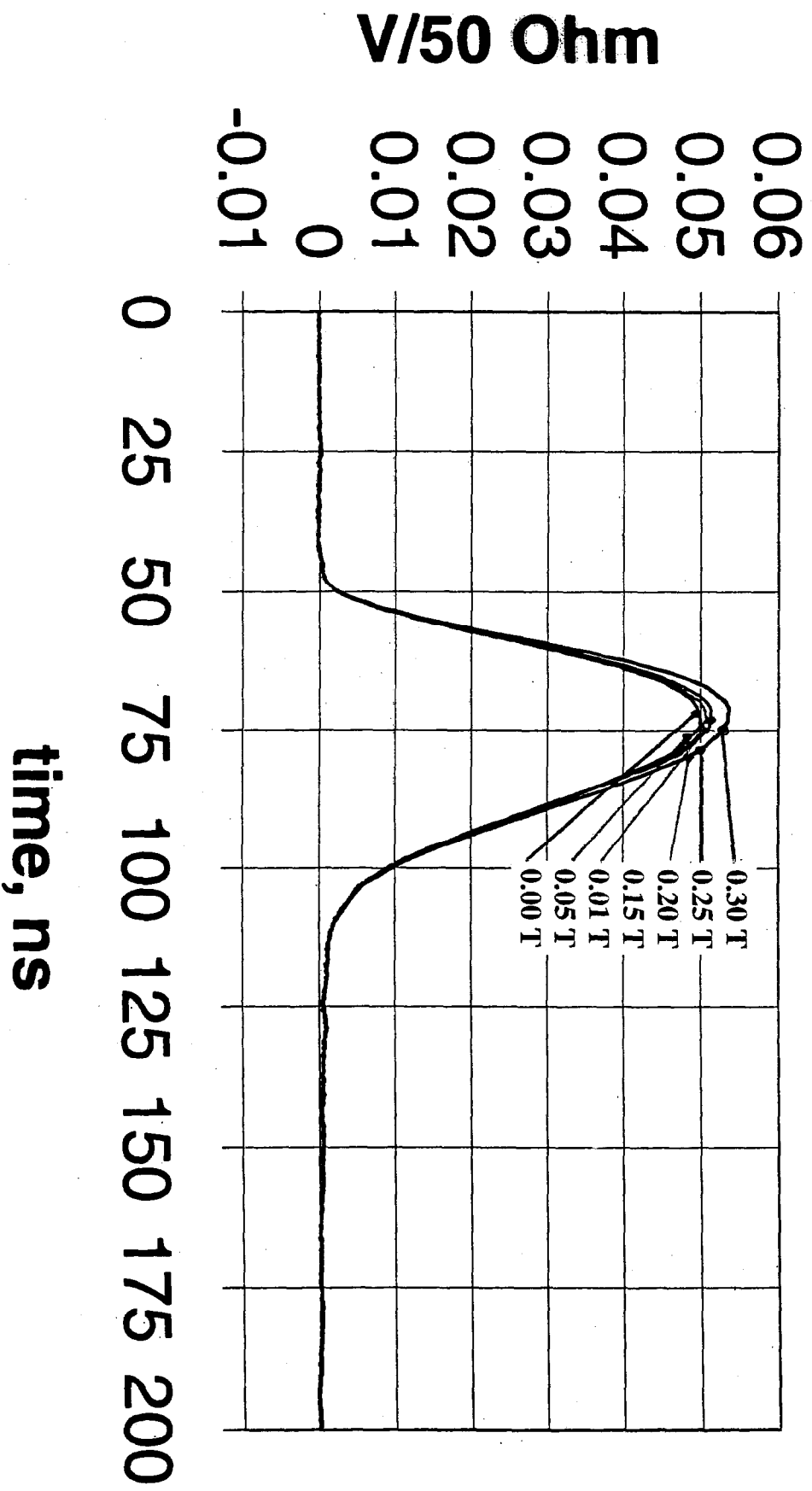


Fig.4

pix11, B variable

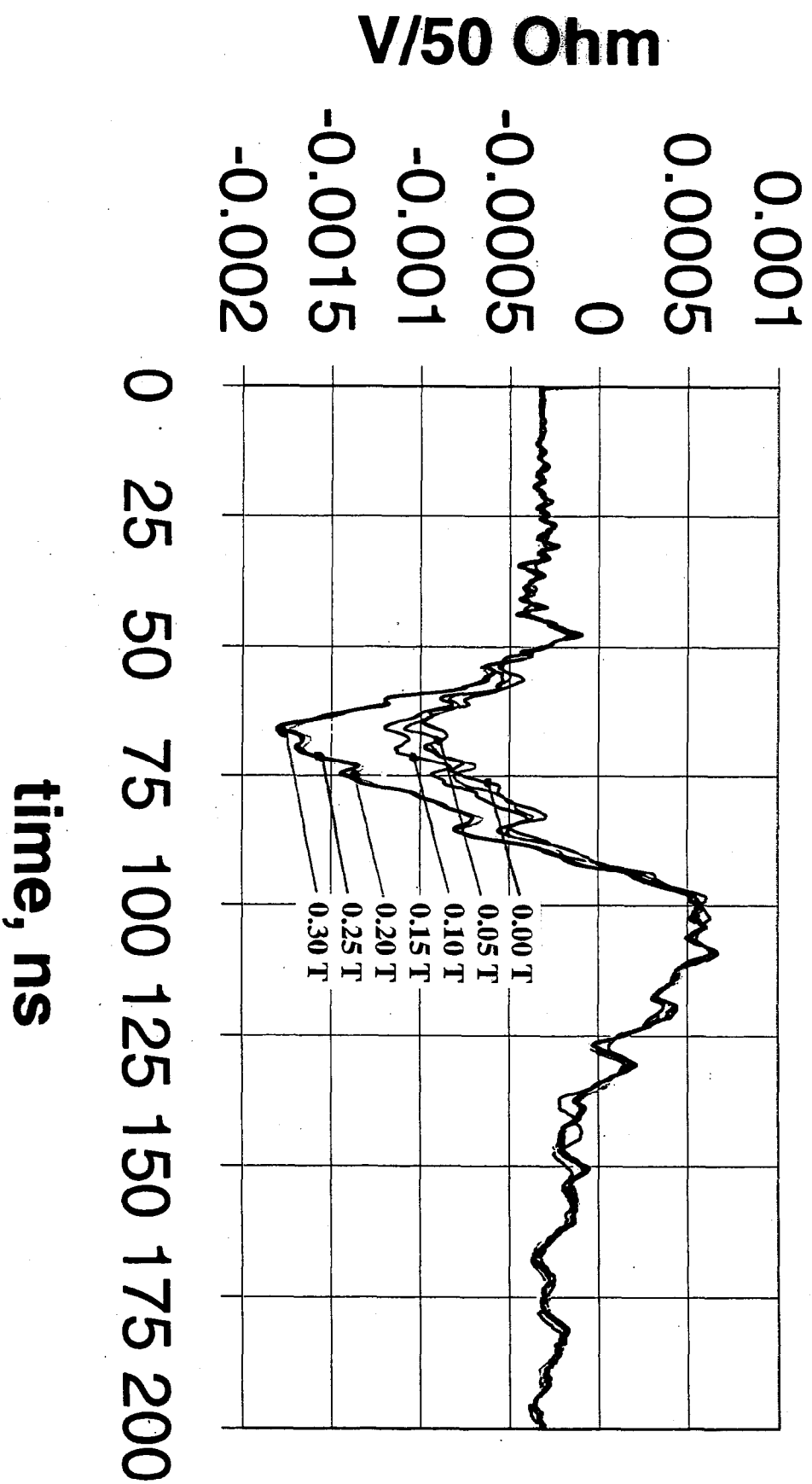


Fig.5

pix12, B variable

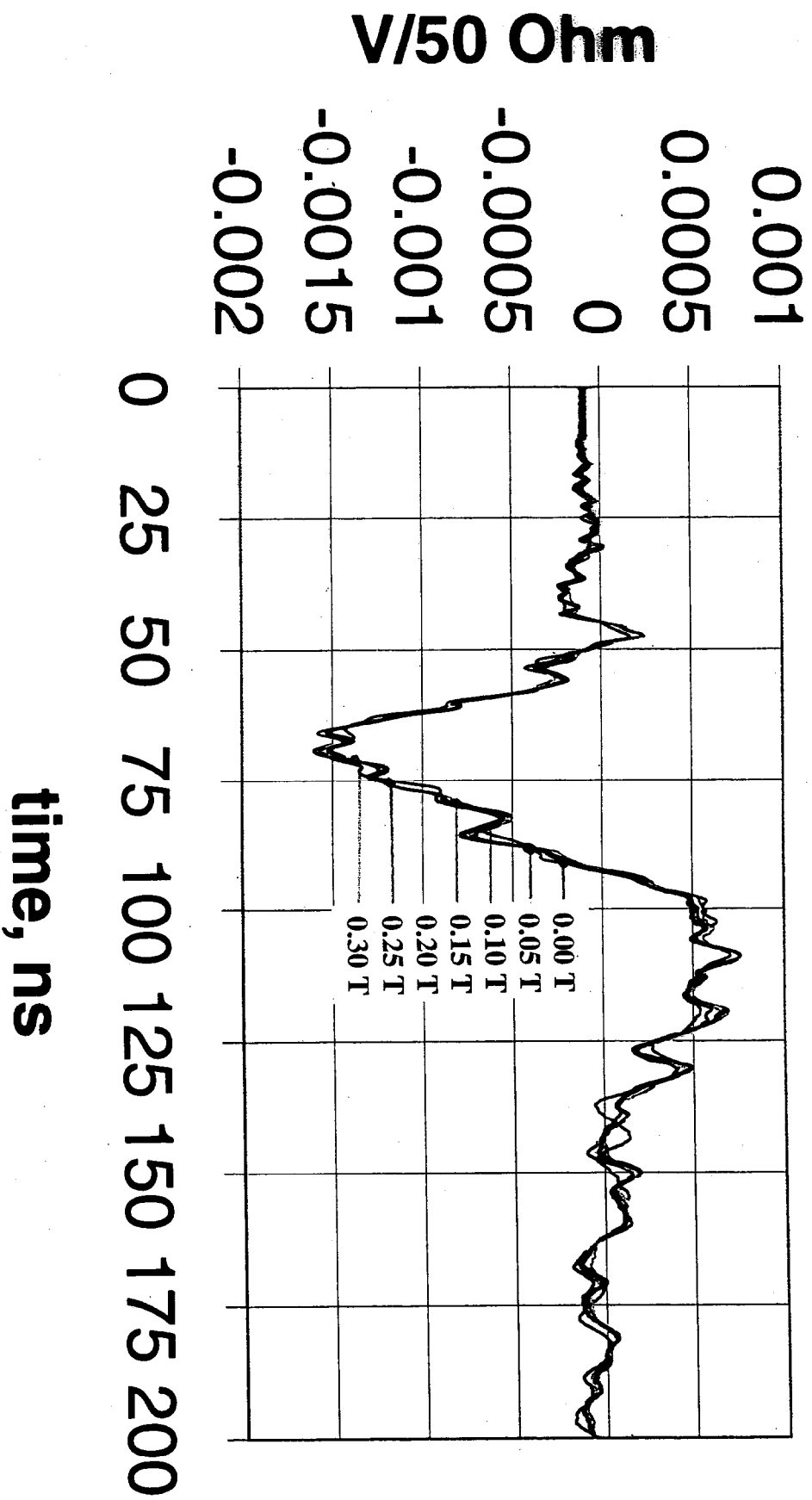


Fig.6

pix 10, B variable

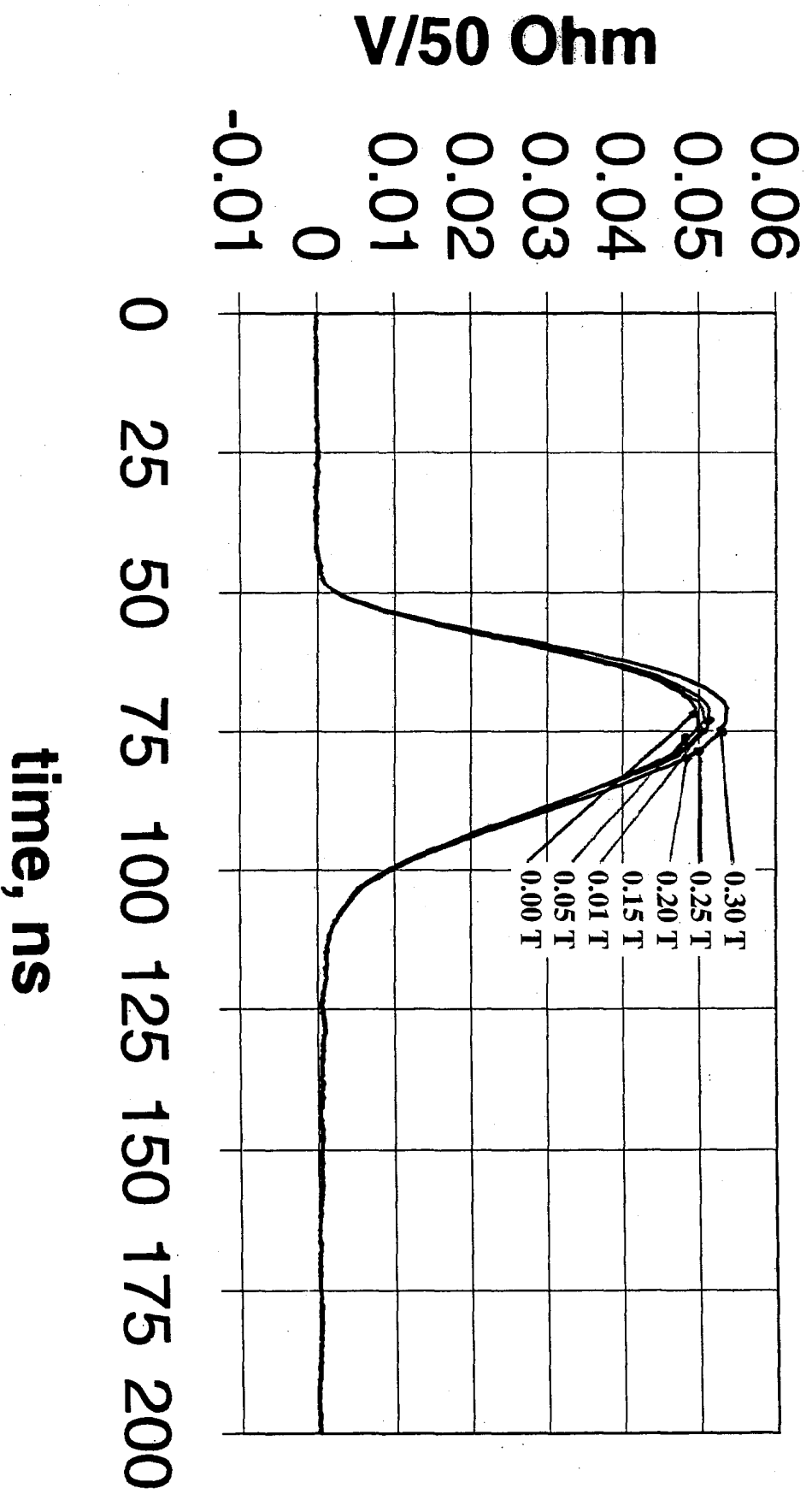


Fig.7

B variable, pix11.

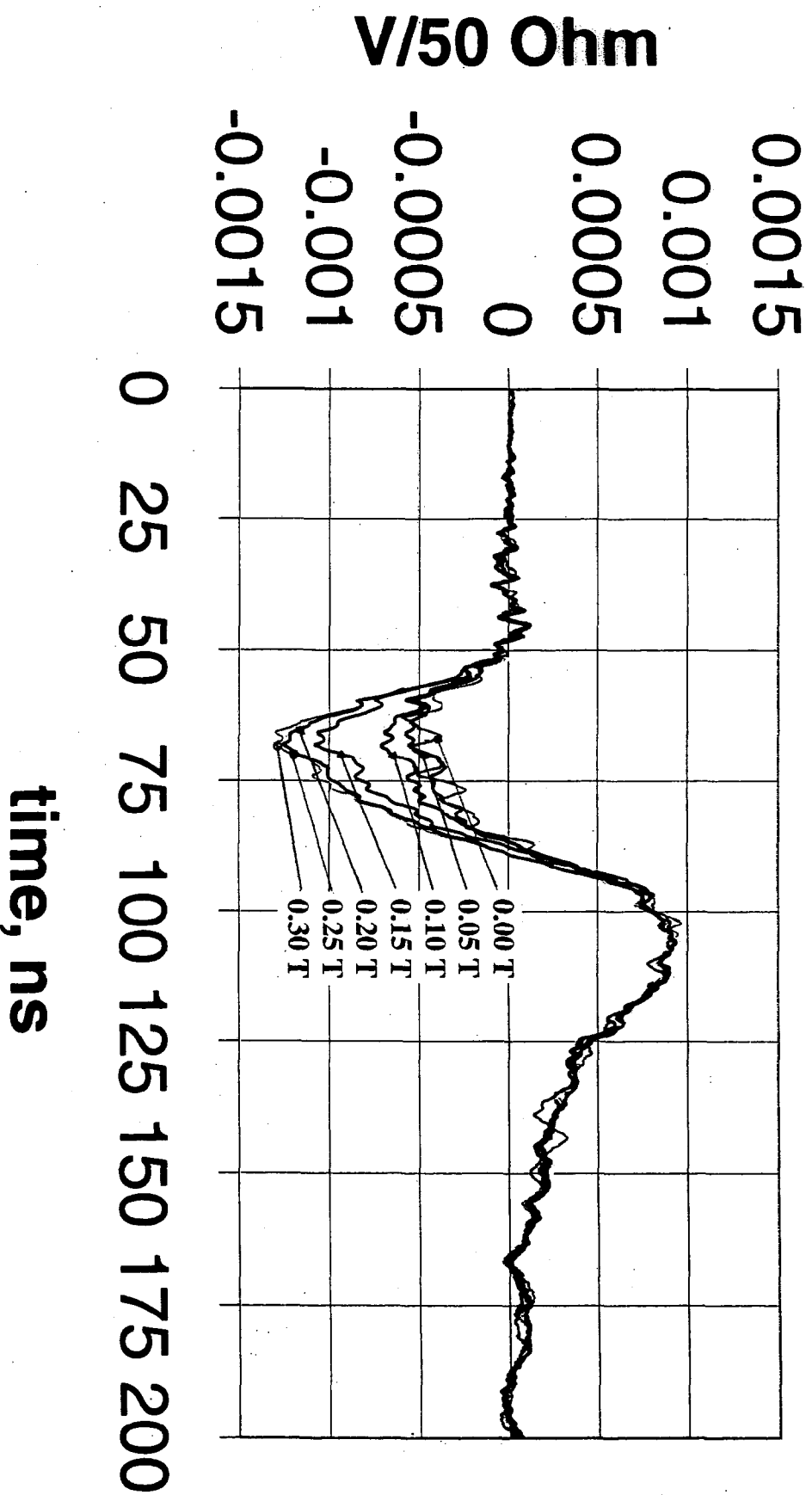


Fig.8

B variable, pix12

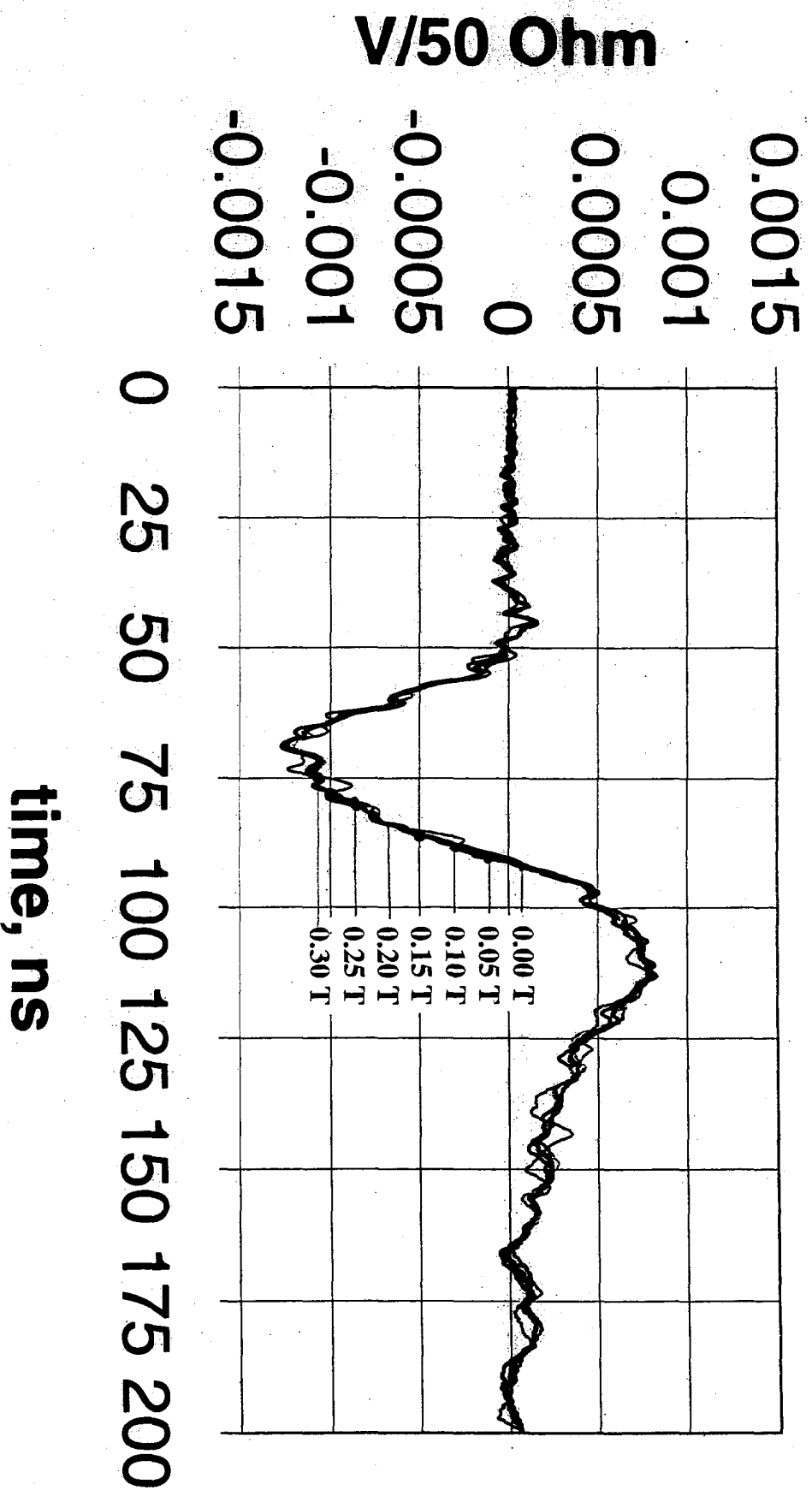


Fig.9

pix 10, B variable

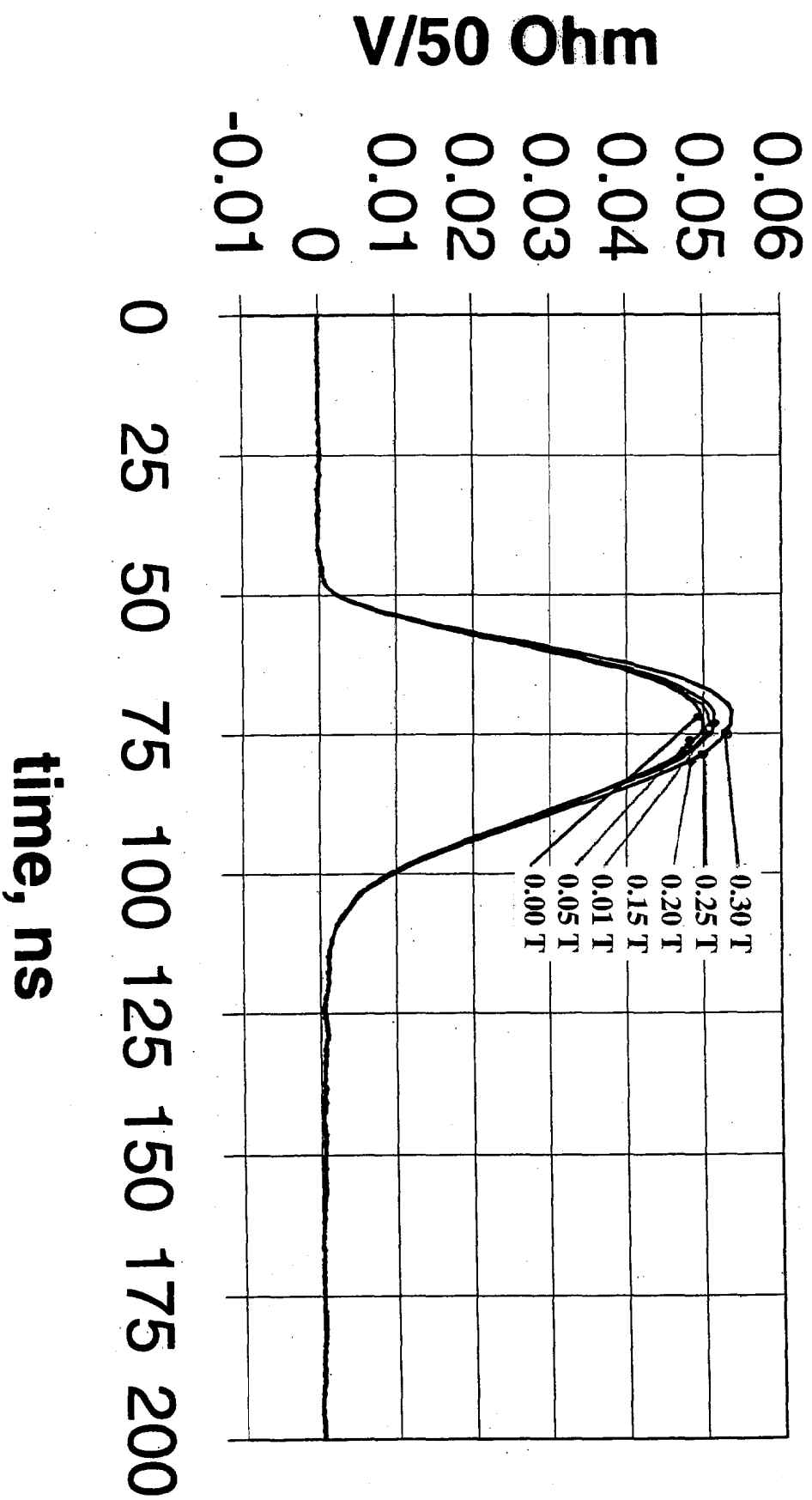


Fig.10

cross on 11 due backsc., B vary

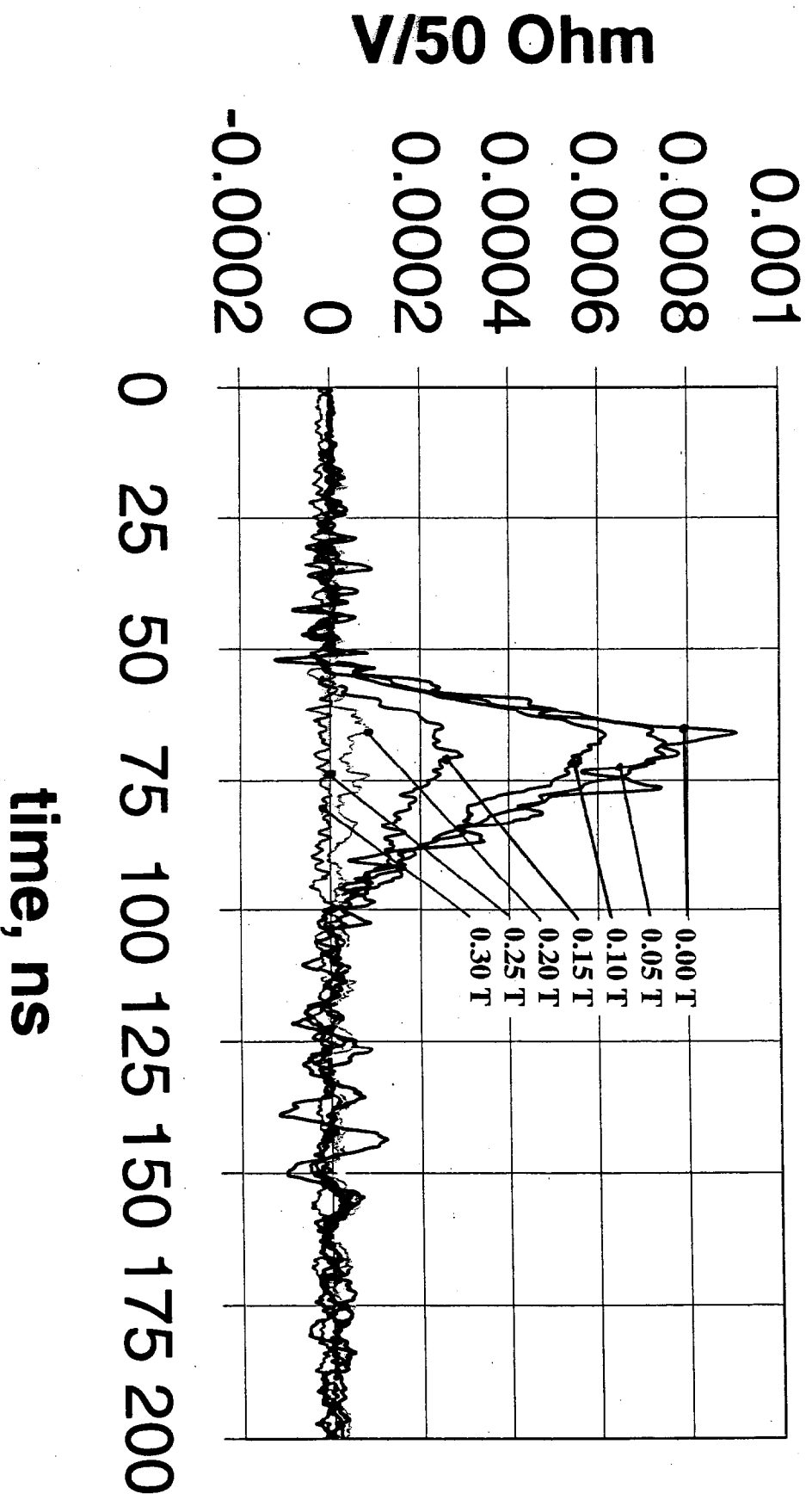


Fig.11

pix 10, B variable

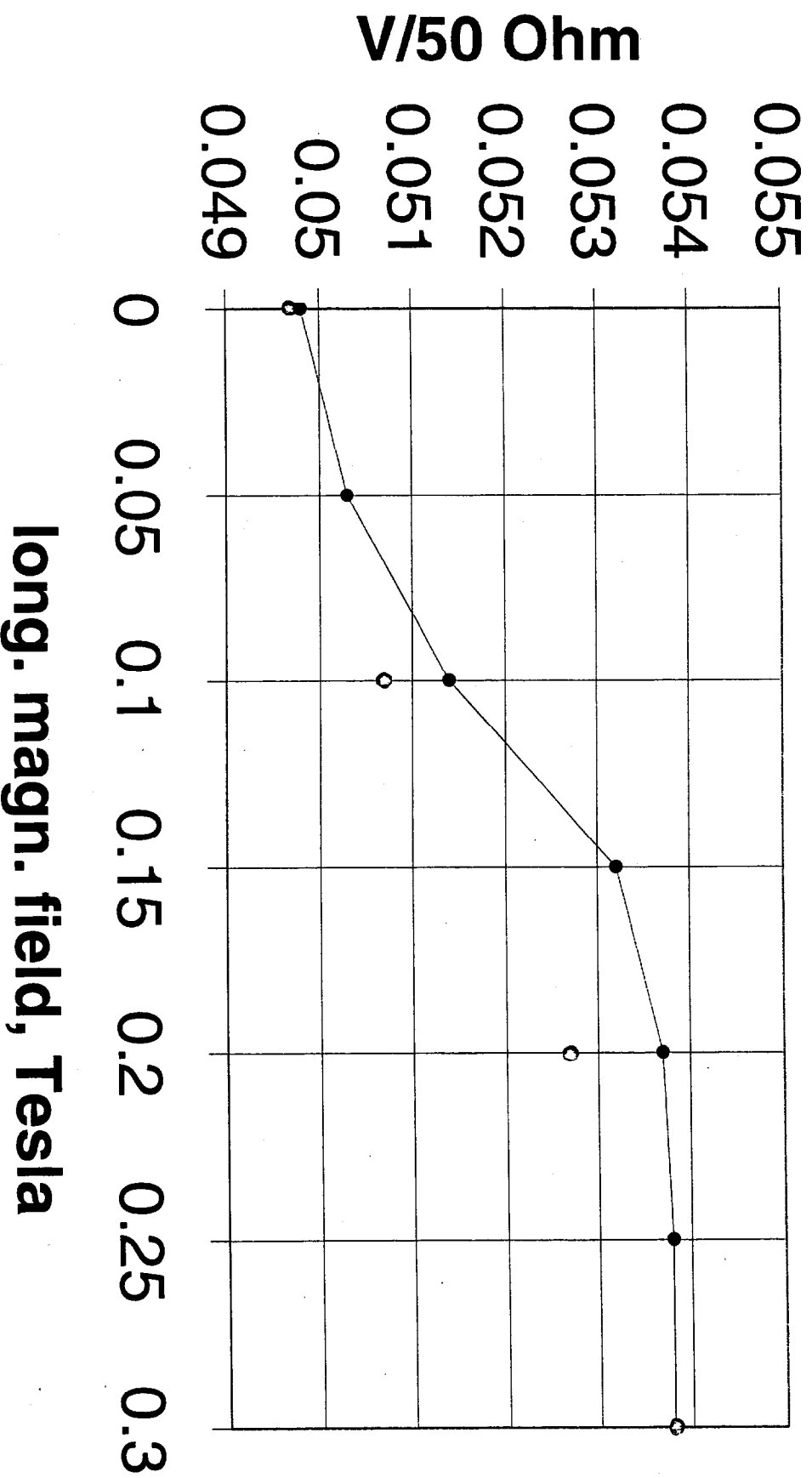


Fig.12

Crosstalk on 11, B variable

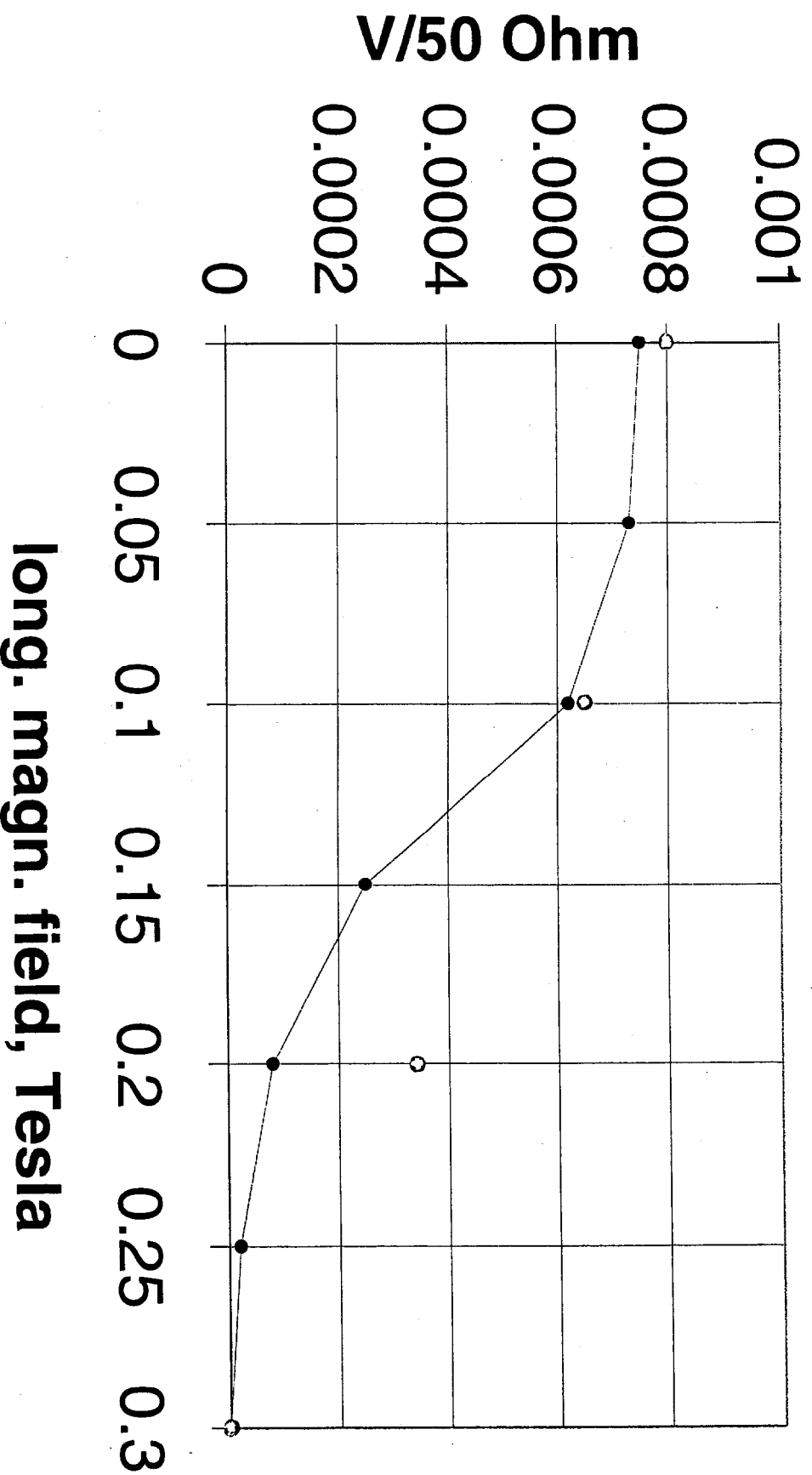


Fig.13

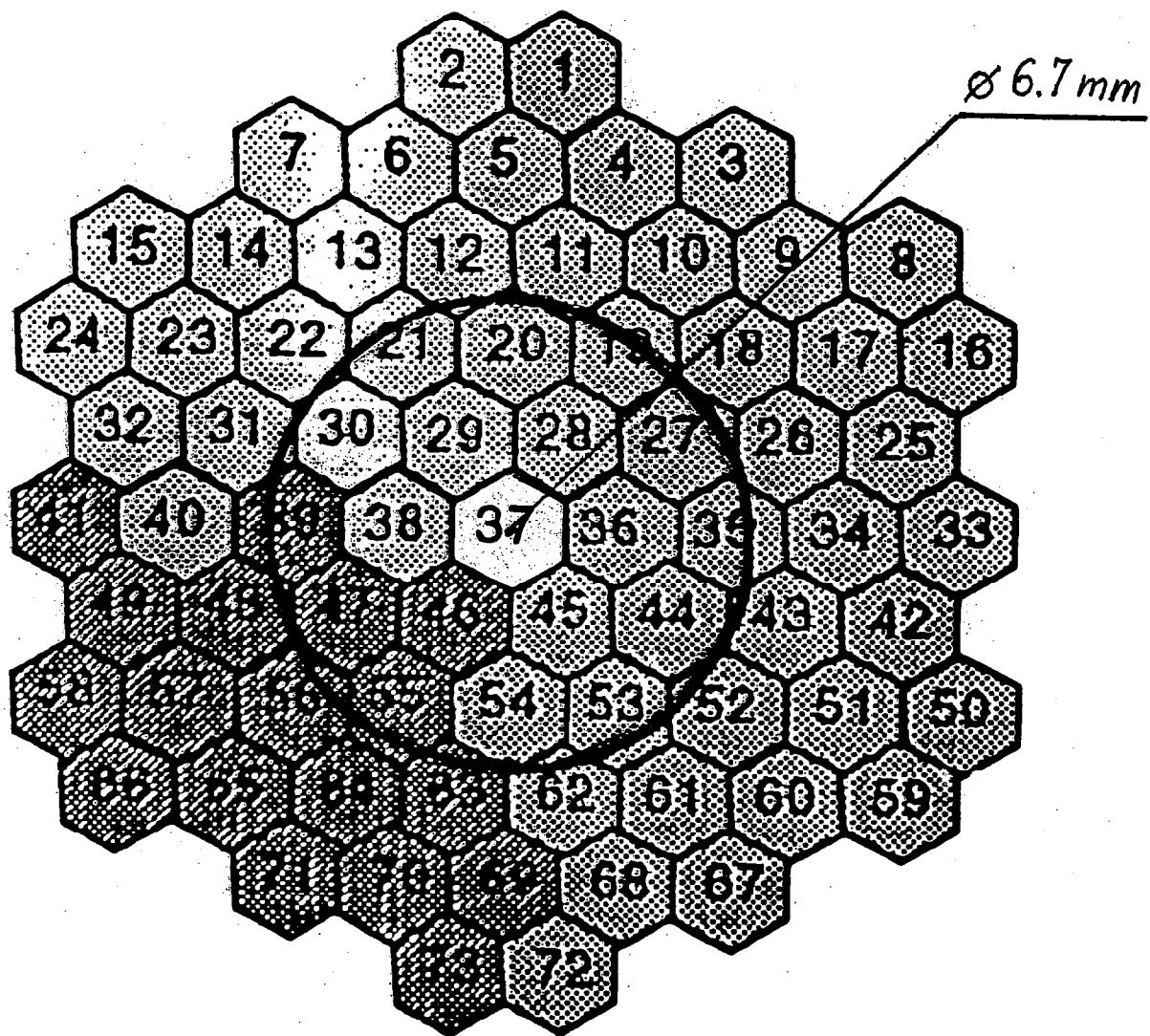


Fig.14

pix 37, B variable

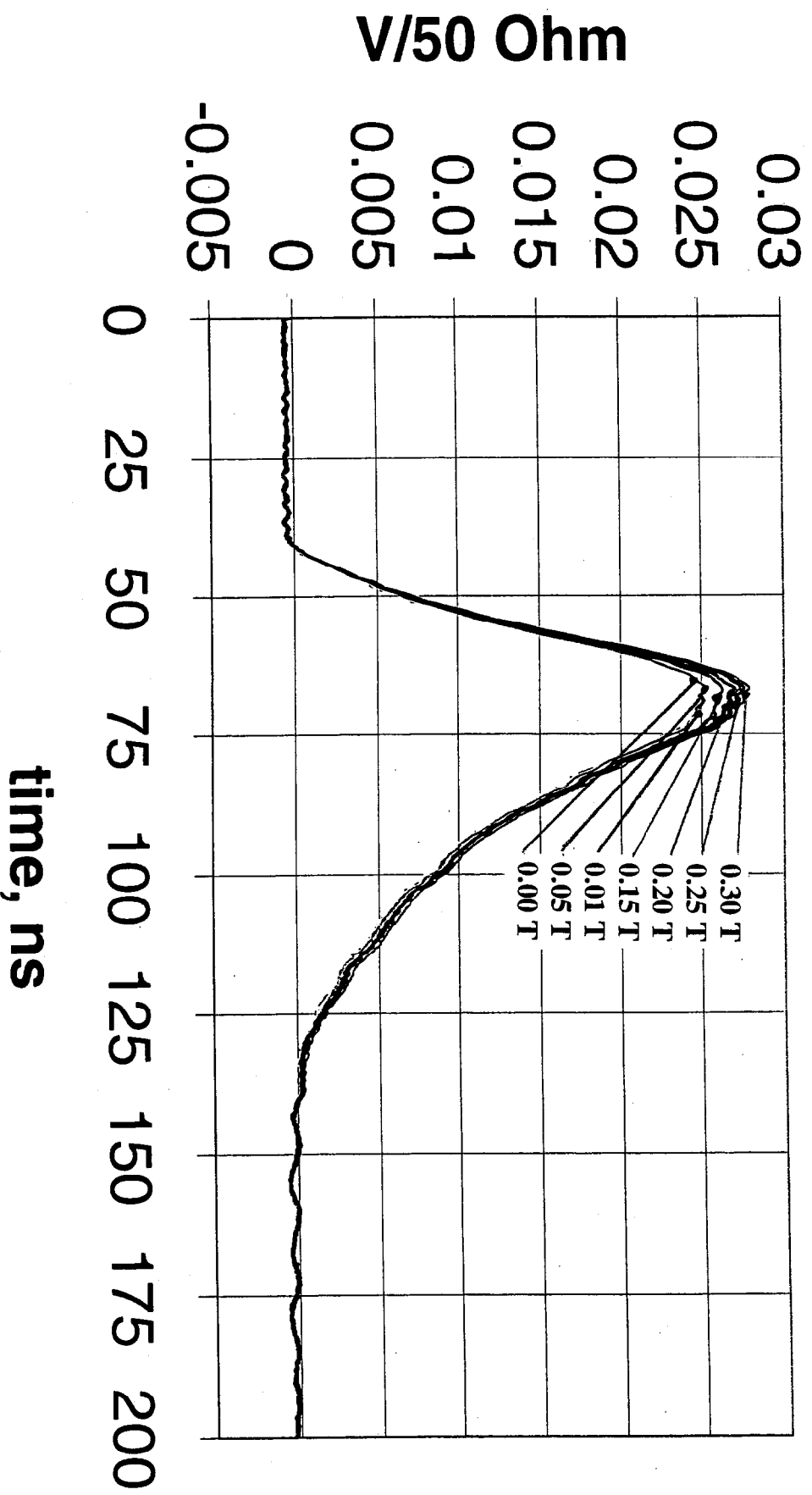


Fig.15

pix 38, B vary

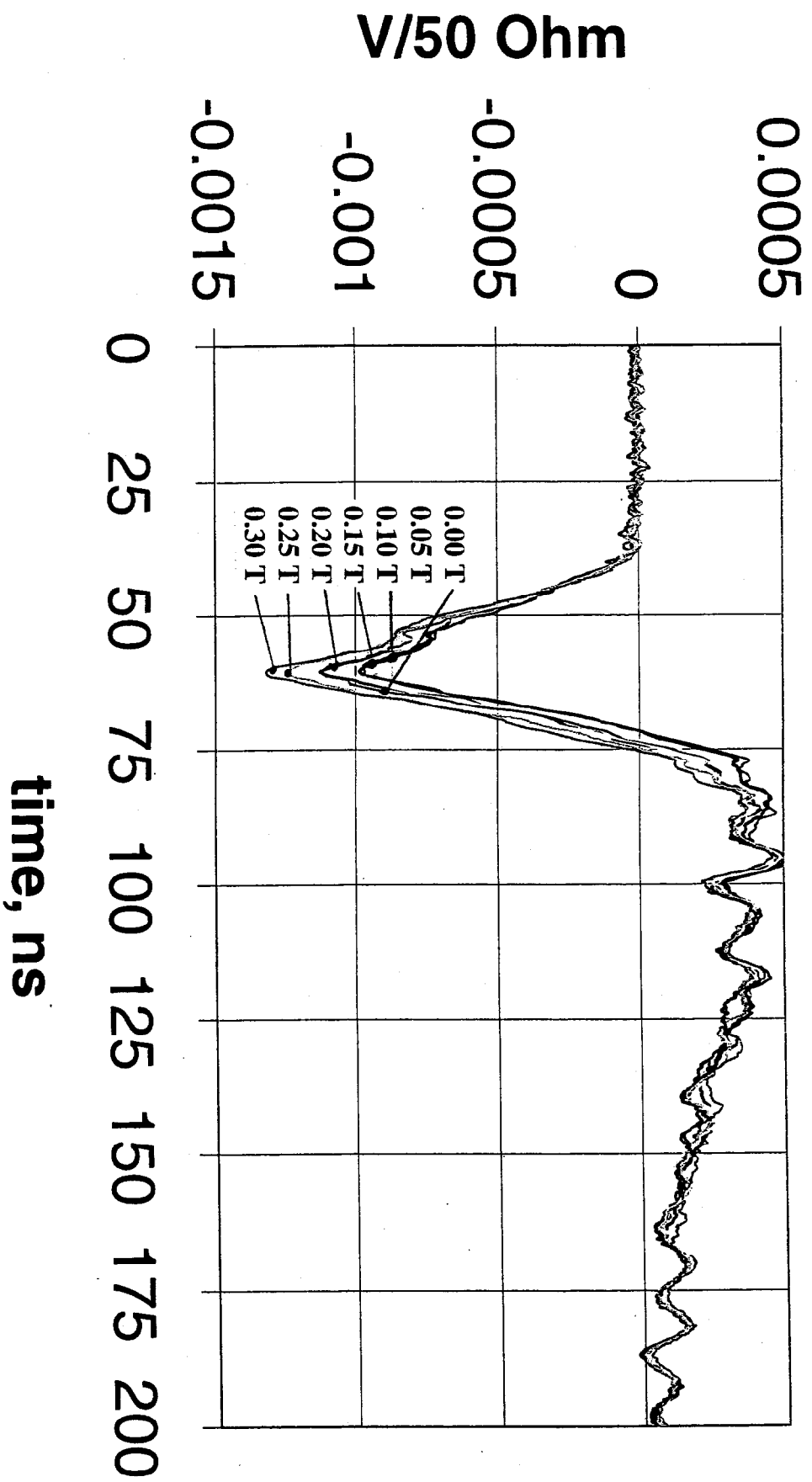


Fig.16

pix 39, B vary

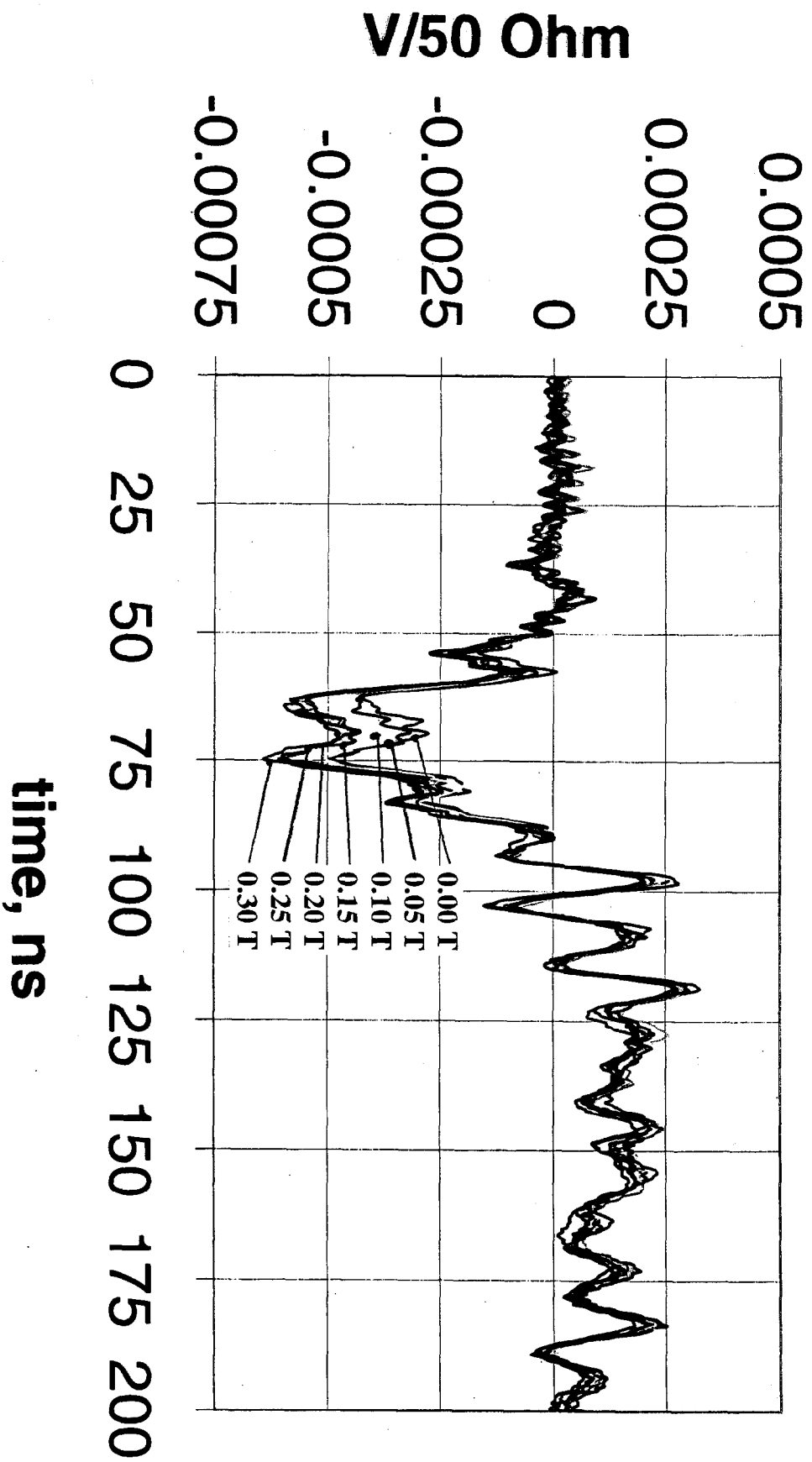


Fig.17

pix 37, B variable

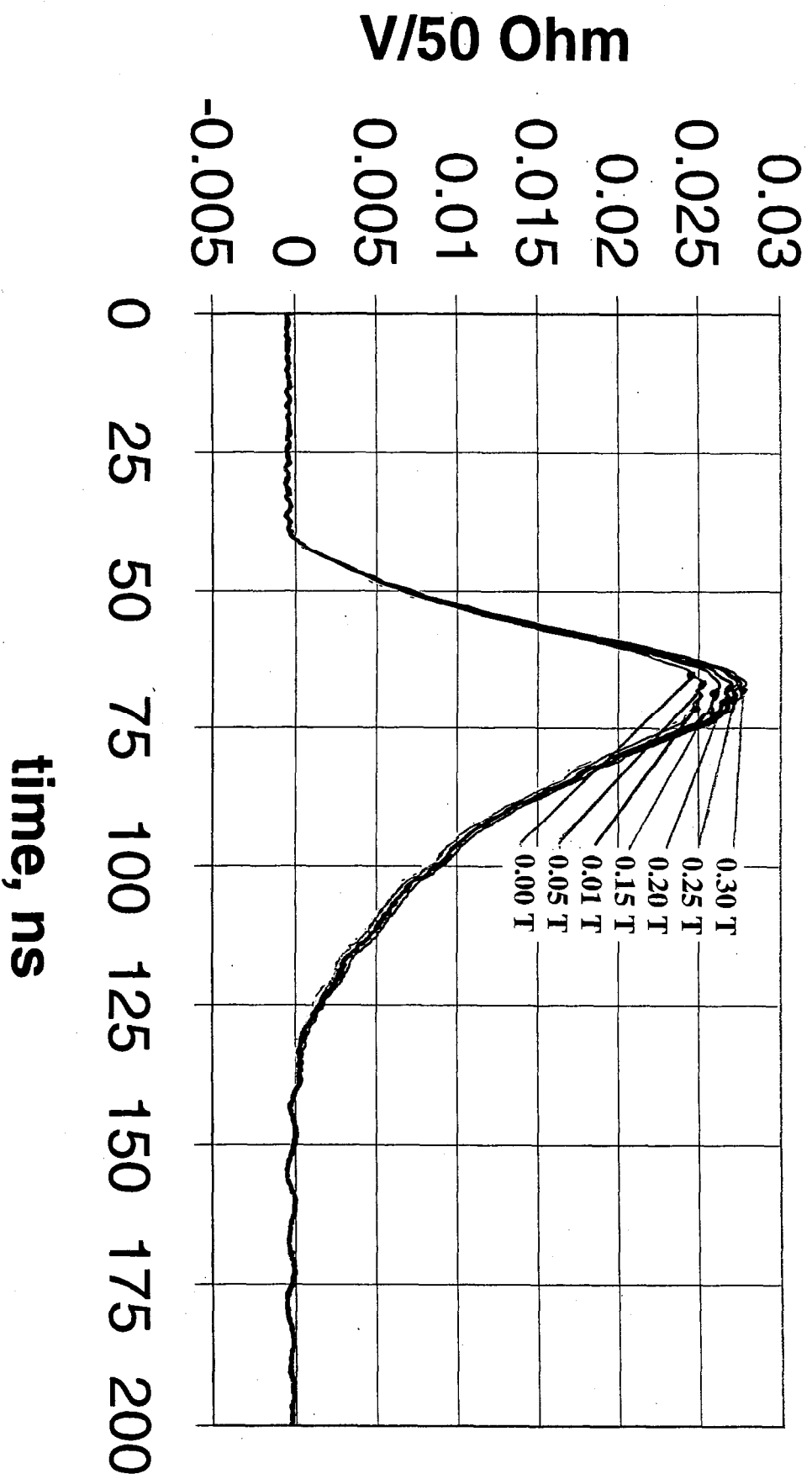


Fig.18

pix 38, B vary

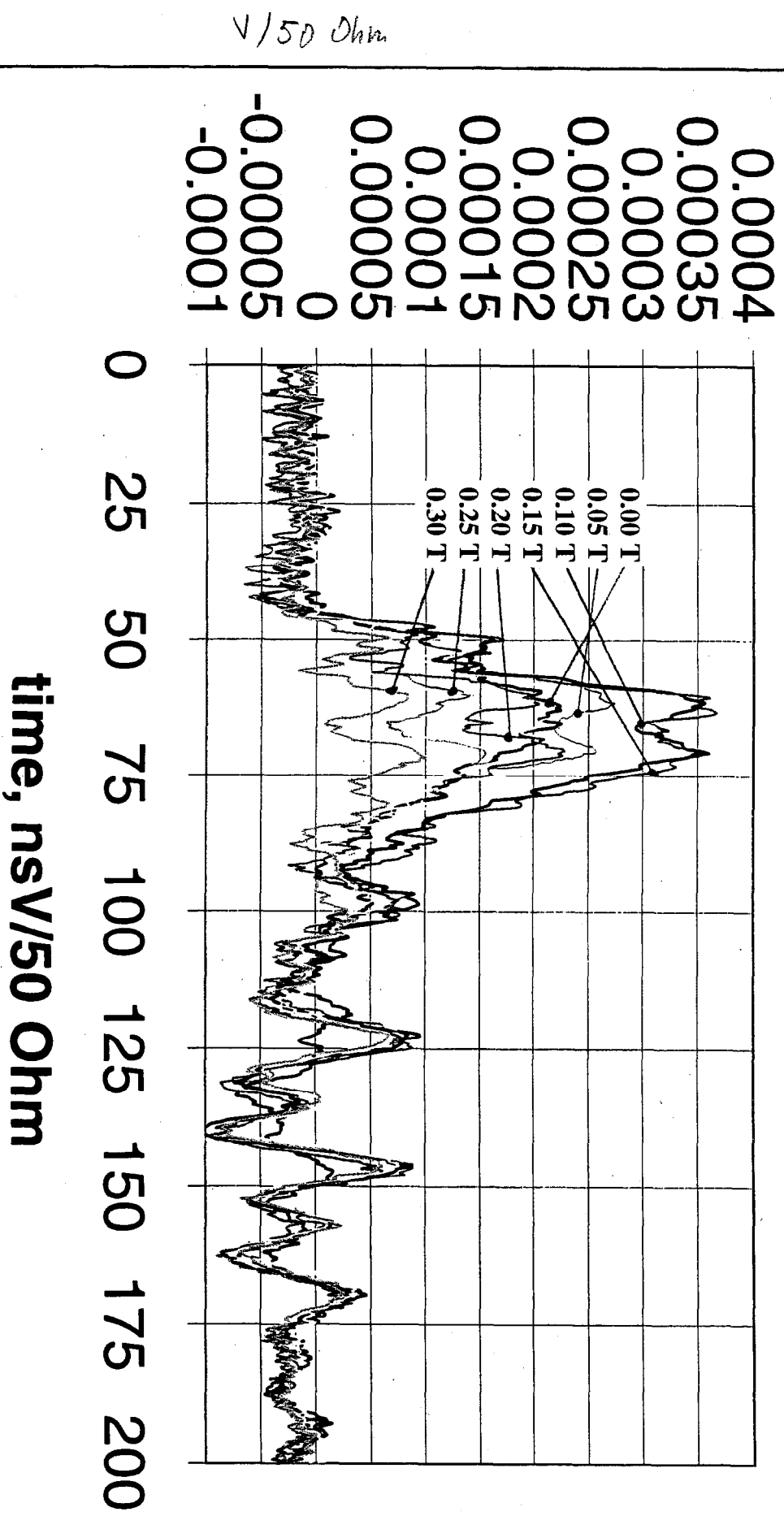


Fig.19

pix 39, B vary

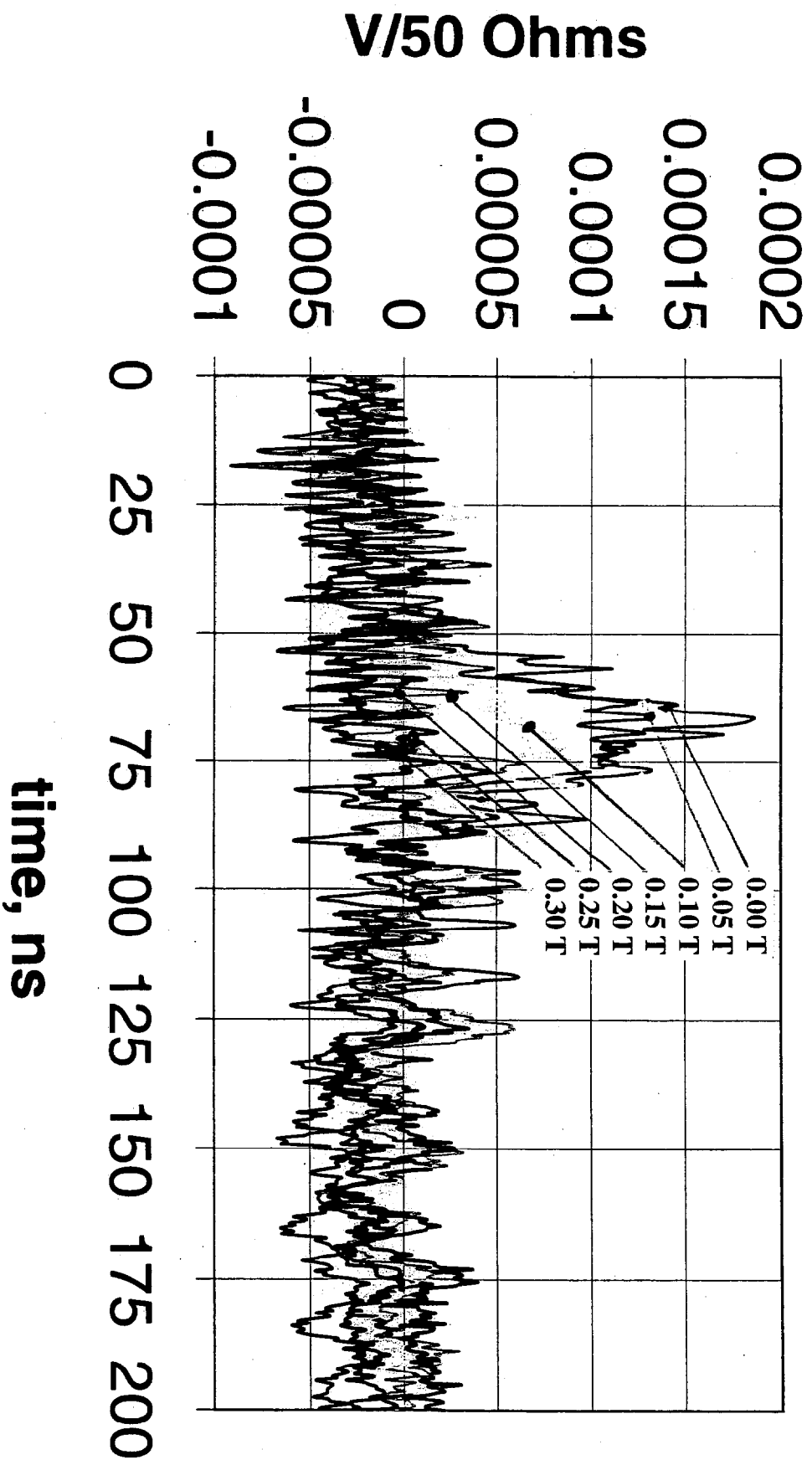


Fig.20

pix 37, B variable

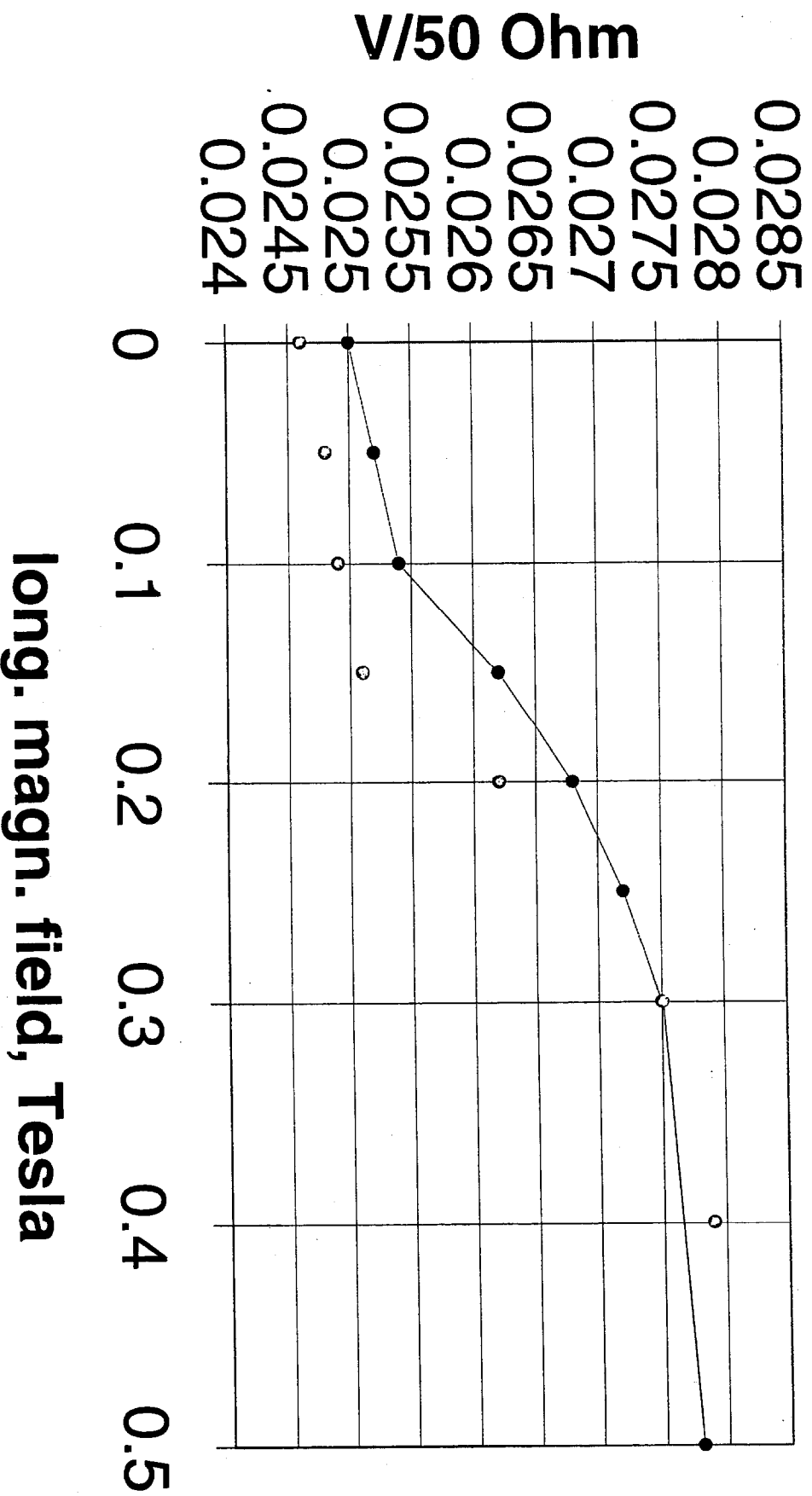


Fig.21

Crasstalk on 38, B variable

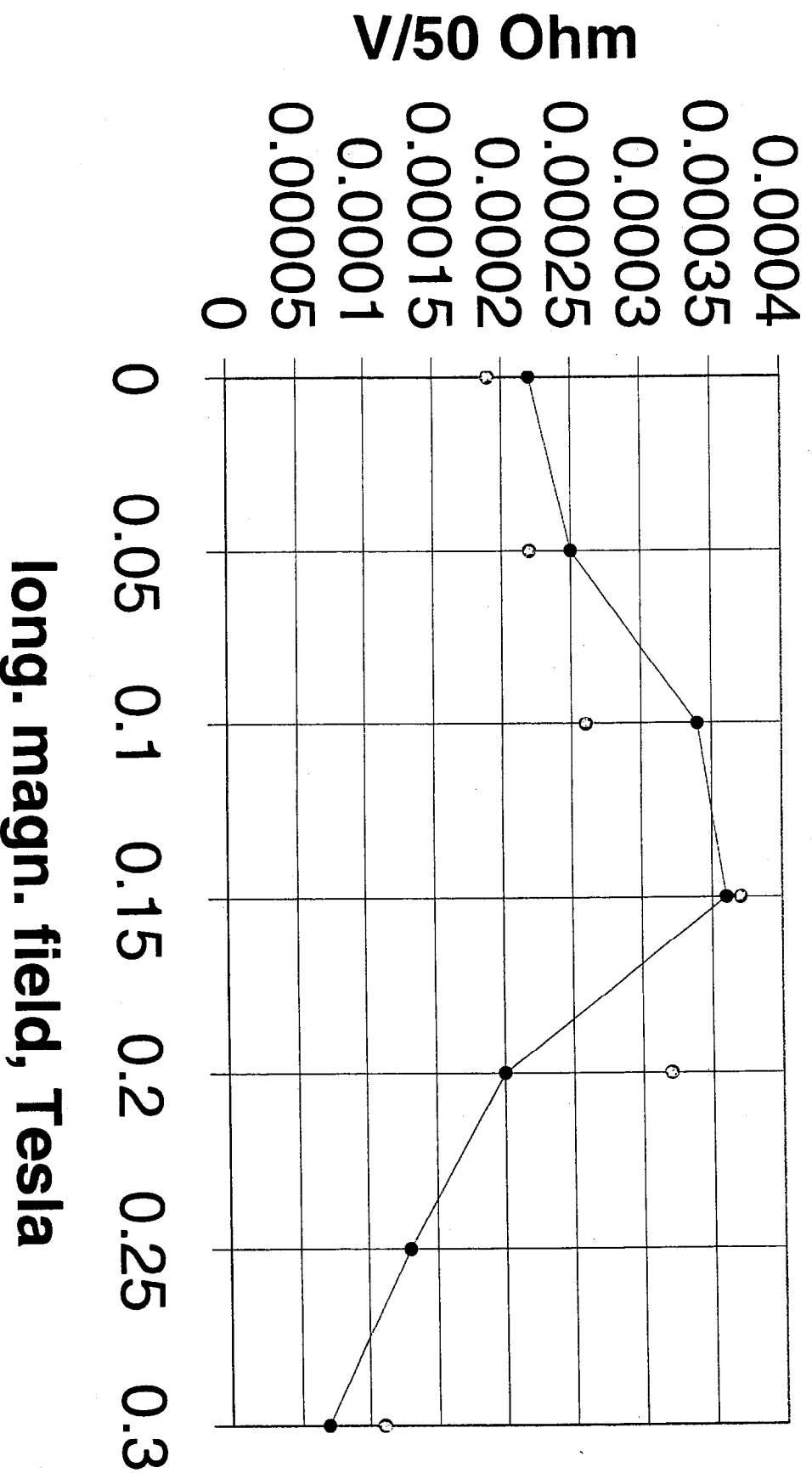


Fig.22

Crosstalk on 39, B variable

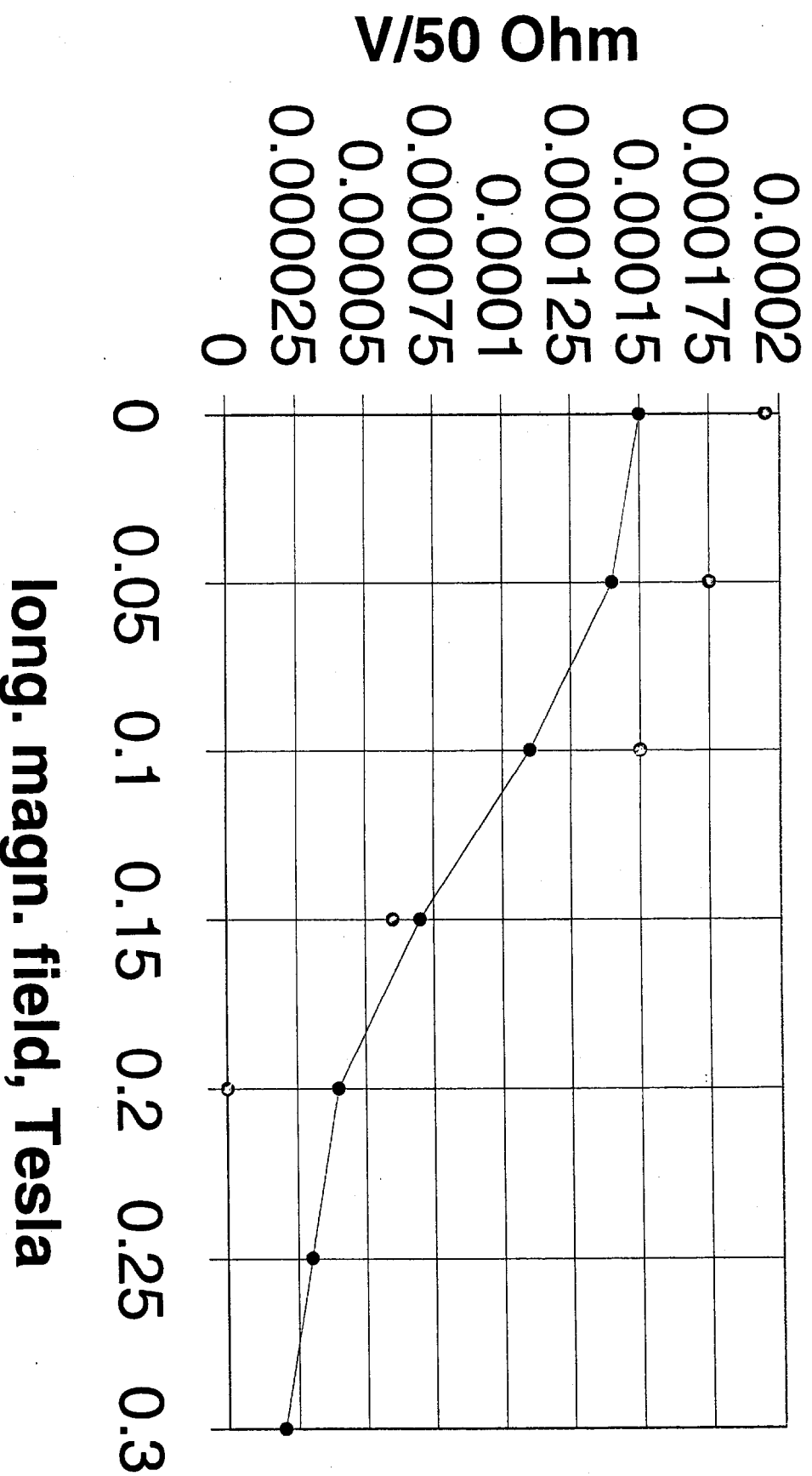


Fig.23